# Alternating mutual influence of El-Niño/Southern Oscillation and Indian monsoon

I. I. Mokhov,[1] D. A. Smirnov,[2,3] P. I. Nakonechny,[3] S. S. Kozlenko,[1] E. P. Seleznev,[2,3] and J. Kurths[4,5]

Received 21 October 2010; accepted 4 November 2010; published 19 January 2011.

[1] Interdependence between El-Niño/Southern Oscillation and Indian monsoon is analyzed with the use of Granger causality estimation from data for the period 1871–2006. Four different versions of the Niño-3 and Niño-3.4 index are used to check robustness of the results. We reveal a non-symmetric bidirectional and even alternating character of coupling that extends previous knowledge about the presence of negative correlation and intervals of phase synchrony between the processes. **Citation:** Mokhov, I. I., D. A. Smirnov, P. I. Nakonechny, S. S. Kozlenko, E. P. Seleznev, and J. Kurths (2011), Alternating mutual influence of El-Niño/Southern Oscillation and Indian monsoon, *Geophys. Res. Lett.*, *38*, L00F04, doi:10.1029/2010GL045932.

## 1. Introduction

[2] Major climatic processes in Asian-Pacific region which are of global importance are related with the phenomena of El-Niño/Southern Oscillation (ENSO) and Indian monsoon [see *Intergovernmental Panel on Climate Change* (*IPCC*), 2007]. The strongest interannual variations in global surface temperature depend on the intensity of the ENSO phenomenon. Significant part of the Earth population lives in the monsoon-related regions with a key role of Indian monsoon. Thus, investigation of the interaction between ENSO and Indian monsoon activity is both of regional and global interest. (Auxiliary material)[1]

[3] The presence of interdependence between these processes has been reliably detected with different techniques [see *Walker and Bliss*, 1932; *Kumar et al.*, 1999; *Maraun and Kurths*, 2005]. Increase in the sea surface temperature (SST) in equatorial Pacific during El-Niño along with the corresponding change in convective processes, the Walker zonal circulation, the Hadley meridional circulation, and the displacement of the intertropical convergence zone, is accompanied by considerable seasonal anomalies of temperature and precipitation in many regions. At that, there are significant variations in the correlation between characteristics of ENSO and Indian monsoon, in particular, its noticeable decrease starting from the last quarter of the XX century [see, e.g., *IPCC*, 2007]. Along with the characterization of an overall coupling strength provided by coherence and synchronization analysis, investigation of the interaction between ENSO and Indian monsoon must involve a quantitative estimation of directional couplings as well as tendencies in their temporal change. In this Letter, we uncover directional coupling characteristics by using the Granger causality, both in its linear and nonlinear versions.

## 2. Data

[4] We have analyzed monthly values of the ENSO and Indian monsoon indices for the period 1871–2006. Indian monsoon is characterized with variations in all-India monthly precipitation [*Mooley and Parthasarathy*, 1984]. As the ENSO index, we use SST in the area Niño-3 (5S-5N, 150W-90W) according to the U.K. Meteorological Office GISST2.3 data for the period 1871–1996 (available at http://badc.nerc.ac.uk/data/gisst/) and Climate Prediction Center data for the period 1997–2006. Other versions of both indices are also compared in Section 4.

[5] Seasonal variations in both processes are related to the insolation cycle. Such an imposed external signal can lead to erroneous conclusions about the presence of mutual influence. Therefore, we remove the seasonal components as follows: (i) a mean value of an index for each calendar month is calculated by averaging over 136 years available; (ii) the monthly mean is subtracted from the observed values corresponding to the respective calendar month. Below, we analyze the deseasonalized signals (Figure 1).

[6] Cross-correlation function and wavelet coherence reveal statistically significant "anti-phase" interdependence between the signals (not shown). However, they do not allow to uncover the character of the coupling, i.e. to find out whether it is unidirectional or bidirectional.

## 3. Method

[7] Granger causality allows to reveal whether the process $x_1$ affects $x_2$ (the influence $1 \rightarrow 2$) and vice versa ($2 \rightarrow 1$) based on the observed time series $x_k(t)$, $t = 1, 2, \ldots, N$, $k = 1, 2$. The approach is based on the construction of univariate and bivariate autoregressive (AR) models and comparison of their prediction errors.

[8] First, one constructs univariate AR-models as

$$x_k(t) = f_k(x_k(t-1), \ldots, x_k(t-d_k)) + \xi_k(t), \qquad (1)$$

where $k = 1, 2$, $d_k$ is a model dimension, $\xi_k$ Gaussian white noise and $f_k$ some function. In the original version

[1]A.M. Obukhov Institute of Atmospheric Physics, Russian Academy of Science, Moscow, Russia.
[2]Saratov Branch, V.A. Kotel'nikov Institute of Radioengineering and Electronics, Russian Academy of Science, Saratov, Russia.
[3]Department of Nano- and Biomedical Technologies, Saratov State University, Saratov, Russia.
[4]Potsdam Institute for Climate Impact Research, Potsdam, Germany.
[5]Institute for Complex systems and Mathematical Biology, University of Aberdeen, UK.


0094-8276/11/2010GL045932

[1]Auxiliary materials are available in the HTML. doi:10.1029/2010GL045932.

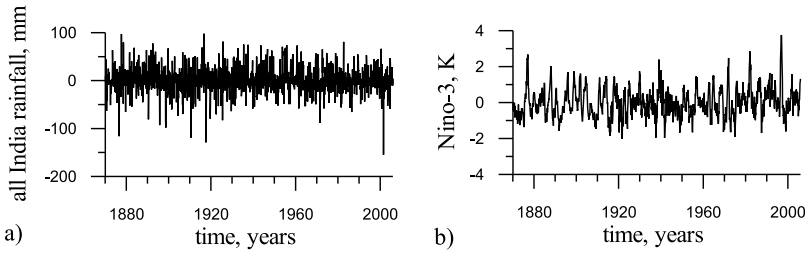


**Figure 1.** The indices of (a) Indian monsoon and (b) ENSO after the removal of the 12-month component.

[*Granger*, 1969] $f_k$ is linear. To describe more complicated processes, nonlinear functions can be used as well. We use algebraic polynomials of an order $L_k$ analogously to [*Mokhov and Smirnov*, 2006]. We did not try other kinds of the function $f_k$ to avoid "in-sample over-optimization". The coefficients of $f_k$ are determined via the least-squares technique, i.e. via minimization of the one-step-ahead mean-squared prediction error of the model. Let us denote its minimal value as $\sigma_k^2$. The latter is an unbiased estimator of the variance of $\xi_k$ in case of sufficiently large $d_k$ and "flexible" $f_k$.

[9] Second, one constructs bivariate AR-models as

$$x_k(t) = f_{k|j}(x_k(t-1),\ldots,x_k(t-d_k),x_j(t-1),\ldots,x_j(t-d_{k|j})) + \eta_k(t). \quad (2)$$

where $j$, $k = 1, 2$, $j \neq k$, $\eta_k$ is Gaussian white noise, $f_{k|j}$ polynomial of the order $L_k$, and additional terms are present as compared to the individual model (1). Namely, $d_{j\to k}$ is the number of $x_j$-values directly "influencing" $x_k$. It characterizes inertial properties of the influence. The model (2) gives a minimal mean-squared prediction error $\sigma_{k|j}^2$. Prediction improvement $PI_{j\to k} = \sigma_k^2 - \sigma_{k|j}^2$ characterizes the causality $j \to k$. Below, we present the normalized values $PI_{j\to k}/\sigma_k^2$. To assess statistical significance of the conclusion about prediction improvement, an $F$-test [*Seber*, 1977] is used. It gives an estimate $p$ of the significance level (the probability of a random error) at which the influence is inferred. We will consider only the values $p < 0.05$ as corresponding to sufficiently reliable conclusions.

[10] The values of $d_k$ are selected based on the Schwarz information criterion [*Schwarz*, 1978], i.e. so to minimize the value of $S_k = \frac{N}{2}\ln\frac{\sigma_k^2}{\mathrm{var}[x_k]} + \frac{P_k}{2}\ln N$, where $\mathrm{var}[x_k]$ is the sample variance of the variable $x_k$, $P_k$ is the number of estimated coefficients of the model (1). To justify an application of the $F$-test, residual errors of the univariate AR-model are checked for delta-correlatedness. Given the value of $d_k$, we select $d_{j\to k}$ and $L_k$ so to obtain the most significant conclusion about the presence of the influence $j \to k$, i.e. to minimize the value of $p$ estimated via the $F$-test. However, the Schwarz criterion gives similar results for the selection of $d_{j\to k}$ and $L_k$. Taking into account optimization over a set of model dimensions, we use the Bonferroni correction to assess significance level of the final conclusion (see below). Validity of the bivariate model is checked by comparing statistical properties of its time realizations to the observed time series $x_k$ ($t$). The values of $d_k$, $d_{j\to k}$, and $L_k$ are sought within such a range that the number of coefficients in any fitted AR-model is less than $\sqrt{N}$.

## 4. Granger Causality Estimates

[11] The monsoon index is further denoted $x_1$ and the ENSO index $x_2$. The analysis of the data for the entire period 1871–2006 gives the following results. For the monsoon index, an optimal individual model is achieved at $d_1 = 1$ and $L_1 = 1$, which gives $\sigma_1^2/\mathrm{var}[x_1] = 0.98$. For the ENSO index, an optimal individual model corresponds to $d_2 = 5$ and $L_2 = 1$. its prediction error is $\sigma_2^2/\mathrm{var}[x_2] = 0.18$. Residual errors of both models are delta-correlated.

[12] Bivariate models for the monsoon index are constructed with $d_1 = 1$ and different values of $L_1$. An optimal model is achieved at $d_{2\to 1} = 1$ and $L_1 = 3$ (Figures 2a and 2c) giving prediction improvement $PI_{2\to 1}/\sigma_1^2 = 0.028$. The conclusion about the presence of the ENSO-to-monsoon influence is highly significant: the pointwise significance level $p$ is of the order of $10^{-8}$, its Bonferroni corrected value is approximately 30 times greater but still very small. The model reads

$$x_1(t) = a_{1,1}x_1(t-1) + b_{1,1}x_2(t-1) + c_{1,1}x_1^2(t-1)x_2(t-1) + c_{1,2}x_2^3(t-1) + \eta_1(t), \quad (3)$$

where $\sigma_{\eta 1}^2 = 5.86 \cdot 10^2$ mm$^2$, coefficients and standard deviations of their estimates [*Seber*, 1977] $a_{1,1} = 0.071 \pm 0.037$, $b_{1,1} = -4.65 \pm 1.11$ mm$\cdot$ K$^{-1}$, $c_{1,1} = (-35.3 \pm 7.59) \cdot 10^{-4}$ mm$^{-1} \cdot$ K$^{-1}$, and $c_{1,2} = 1.53 \pm 0.38$ mm$\cdot$ K$^{-3}$. Only the coefficients different from zero at least at the significance level 0.05 are shown. Optimality of the value of $d_{2\to 1} = 1$ means "inertialless" influence. The linear coupling coefficient $b_{1,1}$ is negative that corresponds to the above mentioned negative correlation between the signals $x_1$ and $x_2$.

[13] A bivariate model for the ENSO index is optimal at $L_2 = 1$ and $d_{1\to 2} = 3$ (Figures 2b and 2d) and gives prediction improvement $PI_{1\to 2}/\sigma_2^2 = 0.024$. The model reads

$$x_2(t) = a_{2,1}x_2(t-1) + a_{2,5}x_2(t-5) + b_{2,1}x_1(t-1) + b_{2,2}x_1(t-2) + b_{2,3}x_1(t-3) + \eta_2(t), \quad (4)$$

where $\sigma_{\eta 2}^2 = 0.11$ K$^2$, $a_{2,1} = 0.92 \pm 0.025$, $a_{2,5} = -0.083 \pm 0.025$, $b_{2,1} = (-1.44 \pm 0.34) \cdot 10^{-3}$ mm$^{-1}$ K, $b_{2,2} = (-1.04 \pm 0.34) \cdot 10^{-3}$ mm$^{-1}$ K, and $b_{2,3} = (-1.01 \pm 0.35) \cdot 10^{-3}$ mm$^{-1}$ K. The monsoon-to-ENSO influence is inertial since $d_{1\to 2} > 1$. Namely, the behavior of the ENSO index depends on the values of the monsoon index for the three previous months. All the three coupling coefficients $b_{2,1}$, $b_{2,2}$, and $b_{2,3}$ do not strongly differ from each other, i.e. the total contribution of

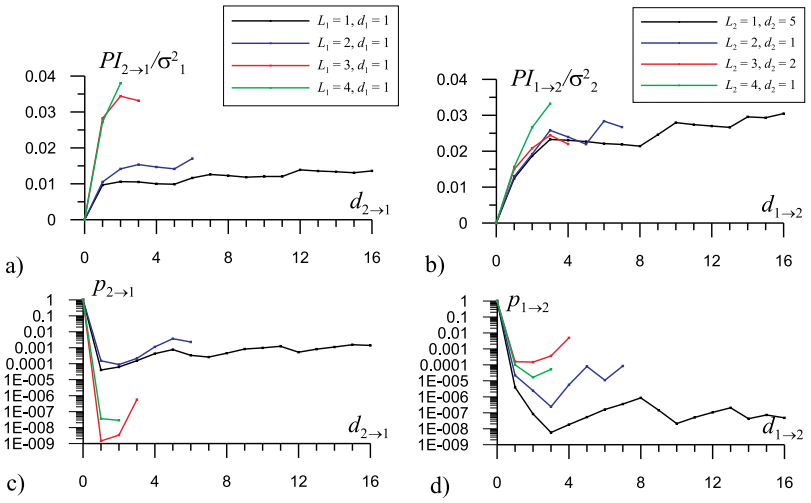


**Figure 2.** (a and b) Prediction improvement and (c and d) significance level for the bivariate models of the monsoon (Figures 2a and 2c) and ENSO (Figures 2b and 2d).

the monsoon index $b_{2,1}x_1(t-1) + b_{2,2}x_1(t-2) + b_{2,3}x_1(t-3)$ is approximately proportional to its average value over three months. No signs of nonlinearity of the monsoon-to-ENSO influence are detected.

[14] We have also used three other versions of the Niño-3 index instead of the GISST data: (i) Kaplan's reconstruction [*Kaplan et al.*, 1998] supplemented with Reynolds' optimal interpolation data [*Reynolds and Smith*, 1994], (ii) Hadley Centre Sea Ice and SST analysis (HADISST) data [*Rayner et al.*, 2003; *Smith et al.*, 2008], (iii) Reynolds' extended reconstructed SST (ERSST) data [*Smith and Reynolds*, 2004; *Smith et al.*, 2008]. In all these versions, anomalies of the Niño-3 SST are available (http://climexp.knmi.nl), where the seasonal component is removed. In general, the results appear quite similar for all the versions of the Niño-3 index. Optimal values of model orders, mean squared prediction errors, and prediction improvements for the entire period 1871–2006 are summarized in Table 1. As one can see, very close values of optimal model dimensions and errors are always obtained. Similar results are obtained if Niño-3.4 index in any version is used instead of the Niño-3 index or All-India Rainfall homogeneous index (http://climexp.knmi.nl) instead of the above monsoon index (not shown). It further confirms robustness of the results.

[15] It is worth noting that different noise levels influencing the monsoon index are observed for different calendar months. Hence, weighted least-squares technique might be more appropriate for the estimation of AR-model coefficients as follows from the maximum likelihood formalism. As we checked, the weighted technique gives almost the same results as reported above. Still, this property of data could be further elaborated: One could perform an analysis separately for the dry and wet months, etc. However, this is beyond the scope of this Letter.

## 5. Coupling Analysis in Moving Window

[16] To trace variations of coupling strengths in time, we have fitted models with parameters indicated in Table 1 to the intervals $[T - W, T]$, where $W$ is the window length and $T$ is a coordinate of the window endpoint. The values of $W$ between 10 and 100 years were checked, the value $W = 30$ gives stable results with a reasonable temporal resolution (Figure 3). To assess significance levels under such analysis, the Bonferroni correction [*Lehmann*, 1986] is applied. Namely, the dashed lines in Figures 3c and 3d show the threshold value of $p_c = 0.05/(N/W)$: If the pointwise

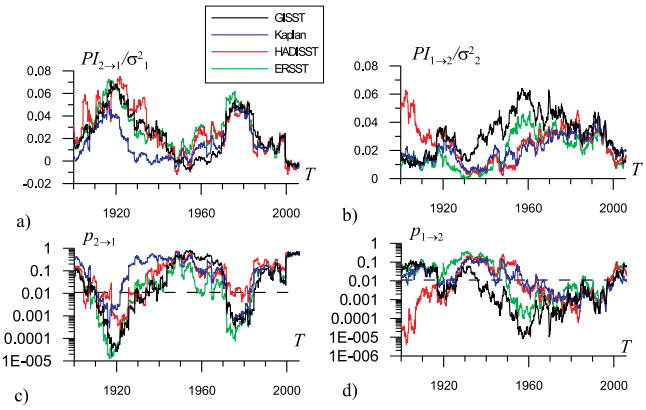


**Figure 3.** (a and c) Estimates of the ENSO-to-monsoon and (b and d) monsoon-to-ENSO influence in a moving window $[T - W, T]$ versus the coordinate of window endpoint $T$ ($W = 30$ years). The dashed lines show Bonferroni corrected pointwise significance levels corresponding to the resulting significance level $p = 0.05$ (see text). Different colors mean the results for different Niño-3 indices.

**Table 1.** Characteristics of Optimal AR-Models for the Entire Period 1871–2006 and Different Versions of the Niño-3 Index

| Data | $d_2$ | $\frac{\hat{\sigma}^2_2}{\mathrm{var}[x_2]}$ | $d_{1\to2}$ | $L_2$ | $\frac{PI_{1\to2}}{\hat{\sigma}^2_2}$ | $d_{2\to1}$ | $L_1$ | $\frac{PI_{2\to1}}{\hat{\sigma}^2_1}$ |
|---|---|---|---|---|---|---|---|---|
| GISST | 5 | 0.18 | 3 | 1 | 0.023 | 1 | 3 | 0.028 |
| Kaplan | 5 | 0.12 | 2 | 1 | 0.021 | 1 | 3 | 0.023 |
| HADISST | 6 | 0.15 | 2 | 1 | 0.022 | 2 | 3 | 0.030 |
| ERSST | 5 | 0.10 | 2 | 1 | 0.016 | 1 | 3 | 0.022 |

significance level $p$ appears less than $p_c$ for a certain time window, we infer the presence of coupling at the resulting significance level less than 0.05 for that window. In this way, ENSO-to-monsoon driving is revealed from the GISST data (Figures 3a and 3c, black lines) for $1910 \le T \le 1930$ and $1975 \le T \le 1985$, i.e. over the intervals 1880–1930 and 1945–1985. Significant monsoon-to-ENSO driving is detected from the GISST data (Figures 3b and 3d, black lines) for $1917 \le T \le 1927$ and, especially, for $1935 \le T \le 2000$. The intervals of the strongest ENSO-to-monsoon and monsoon-to-ENSO driving do not coincide in time but follow each other.

[17] Different colors in Figure 3 denote the results for different Niño-3 indices. The ENSO-to-monsoon coupling strength exhibits the same temporal evolution for any Niño-3 index (Figures 3a and 3c). Slight differences are seen for the opposite direction (Figures 3b and 3d). Namely, GISST and ERSST indices show that the monsoon-to-ENSO influence is maximal around 1950–1960, while the two other indices suggest its maximality around 1980–1990. Moreover, the HADISST data show an additional period of strong monsoon-to-ENSO driving in 1870–1905. Thus, an alternating character of ENSO-monsoon coupling is seen from any Niño-3 index. However, GISST and ERSST data suggest a more interesting pattern of alternating epochs of almost unidirectional ENSO-to-monsoon or monsoon-to-ENSO couplings. Some differences between the plots in Figure 3 for different versions of the Niño-3 index in the early periods may be due to different pre-processing that can influence the PI estimates.

[18] It was discussed by *Gershunov et al.* [2001] that variations of correlation coefficient estimates under the moving windows analysis may result purely from random fluctuations even for constant couplings. Similarly to that work, we checked statistical significance of our conclusions about variable character of couplings by surrogate data tests. Namely, an ensemble of time series of the length of 1632 steps was generated by an optimal bivariate model with constant couplings (Table 1). Each simulated time series was processed exactly as the climatic data above. From each obtained realization $PI_{i\to j}(t)$ the standard deviation $\sigma_{PIi\to j}$ was calculated. 0.95-quantile of this quantity $\sigma^{(0.95)}_{PIi\to j}$ was determined. The values $\sigma_{PIi\to j}$ for the climatic data appeared greater than the respective $\sigma^{(0.95)}_{PIi\to j}$ for both directions and each version of the Niño-3 index. E.g., for the GISST data we got $\sigma_{PI2\to 1} = 0.02$, $\sigma^{(0.95)}_{PI2\to 1} = 0.008$ and $\sigma_{PI1\to 2} = 0.014$, $\sigma^{(0.95)}_{PI1\to 2} = 0.005$. Thus, the observed fluctuations of the Granger causality characteristics (Figure 3) are statistically significant at least at the significance level $p < 0.05$.

## 6. Conclusions

[19] Based on the Granger causality analysis, we have obtained characteristics of interaction between ENSO and Indian monsoon which complement previously known results about their anti-correlation [*Walker and Bliss*, 1932] and phase synchrony intervals [*Maraun and Kurths*, 2005].

[20] For any version of the Niño-3 and Niño-3.4 index used in this work, bidirectional coupling between ENSO and Indian monsoon is detected with high confidence. The ENSO-to-monsoon influence is inertialless and nonlinear. The monsoon-to-ENSO influence is linear and inertial: the values of the monsoon index for two or three months affect the future behavior of the ENSO index. It is interesting to note that in model simulations [*Wu and Kirtman*, 2003] almost instantaneous ENSO-to-monsoon influence and 6-month lagged backward influence were observed, which is in some respect similar to the above results of data analysis. Moving window analysis reveals an alternating character of the coupling. ENSO-to-monsoon influence is strongest during the period of 1890–1920. It is also noticeable in 1950–1980 and not detected in 1920–1950 and after 1980. The monsoon-to-ENSO coupling also varies in time, but in somewhat different ways for different versions of the Niño-3 index. As for the geophysical interpretation, possible mechanisms of the influence of the monsoon system on ENSO are discussed in different publications. For instance, changes in the monsoon system can influence the trade winds in the Pacific and, hence, affect the ENSO characteristics.

[21] The results about variable and bidirectional character of the ENSO – Indian monsoon coupling must be helpful for the understanding of the mechanism behind this interaction.

[22] **Acknowledgments.** The authors thank B. Knopf and H.J. Schellnhuber for important suggestions. The work is supported by the Russian Foundation for Basic Research, Programs of RAS and Russian Ministry of Education and Science. J.K. acknowledges support from DFG Graduate School 1364 and EU-Project SUMO.

## References

Gershunov, A., N. Schneider, and T. Barnett (2001), Low frequency modulation of the ENSO-Indian monsoon rainfall relationship: Signal or noise, *J. Clim.*, *14*, 2486–2492.

Granger, C. W. J. (1969), Investigating causal relations by econometric models and cross-spectral methods, *Econometrica*, *37*, 424–438.

Intergovernmental Panel on Climate Change (IPCC) (2007), *Climate Change* 2007*: The Physical Science Basis: Contribution I to the Fourth Assessment Report of the Intergovernmental Panel on Climate Change*, edited by S. Solomon et al., Cambridge University Press, New York.

Kaplan, A., M. Cane, Y. Kushnir, A. Clement, M. Blumenthal, and B. Rajagopalan (1998), Analyses of global sea surface temperature 1856–1991, *J. Geophys. Res.*, *103*, 18,567–18,589.

Kumar, K. K., B. Rajagopalan, and A. M. Cane (1999), On the weakening relationship between the Indian monsoon and ENSO, *Science*, *284*, 2156–2159.

Lehmann, E. (1986), *Testing Statistical Hypothesis*, Springer, Berlin.

Maraun, D., and J. Kurths (2005), Epochs of phase coherence between El Niño/Southern Oscillation and Indian monsoon, *Geophys. Res. Lett.*, *32*, L15709, doi:10.1029/2005GL023225.

Mokhov, I. I., and D. A. Smirnov (2006), El Niño-Southern Oscillation drives North Atlantic Oscillation as revealed with nonlinear technique from climatic indices, *Geophys. Res. Lett.*, *33*, L03708, doi:10.1029/2005GL024557.

Mooley, D. A., and B. Parthasarathy (1984), Fluctuations in all-India summer monsoon rainfall during 1871–1978, *Clim. Change*, *6*, 287–301.

Rayner, N. A., D. E. Parker, E. B. Horton, C. K. Folland, L. V. Alexander, D. P. Rowel, E. C. Kent, and A. Kaplan (2003), Global analyses of sea surface temperature, sea ice, and night marine air temperature since the late nineteenth century, *J. Geophys. Res.*, *108*(D14), 4407, doi:10.1029/2002JD002670.

Reynolds, R. W., and T. M. Smith (1994), Improved global sea surface temperature analyses, *J. Clim.*, *7*, 929–948.

Schwarz, G. (1978), Estimating the order of a model, *Ann. Stat.*, *6*, 461–464.

Seber, G. A. F. (1977), *Linear Regression Analysis*, Wiley, New York.

Smith, T. M., and R. W. Reynolds (2004), Improved extended reconstruction of SST (1854–1997), *J. Clim.*, *17*, 2466–2477.

Smith, T. M., R. W. Reynolds, T. C. Peterson, and J. Lawrimore (2008), Improvements to NOAA's historical merged land–ocean surface temperature analysis (1880–2006), *J. Clim.*, *21*, 2283–2296.

Walker, G. T., and E. W. Bliss (1932), World weather V, *Mem. R. Meteorol. Soc.*, *4*, 3–84.

Wu, R., and B. P. Kirtman (2003), On the impacts of the Indian summer monsoon on ENSO in a coupled GCM, *Q. J. R. Meteorol. Soc.*, *129*, 3439–3468.

S. S. Kozlenko and I. I. Mokhov, A.M. Obukhov Institute of Atmospheric Physics, Russian Academy of Science, Pyzhevsky 3, Moscow 119017, Russia. (kozlenko@ifaran.ru; mokhov@ifaran.ru)

J. Kurths, Potsdam Institute for Climate Impact Research, Telegraphenberg PO Box 601203, D-14412 Potsdam, Germany. (kurths@pik-potsdam.de)

P. I. Nakonechny, Department of Nano- and Biomedical Technologies, Saratov State University, Astrakhanskaya Str. 83, Saratov 410012, Russia. (zorg1331@gmail.com)

E. P. Seleznev and D. A. Smirnov, Saratov Branch, V.A. Kotel'nikov Institute of Radioengineering and Electronics, Russian Academy of Science, Zelyonaya Str. 38, Saratov 410019, Russia. (seleznev@sgu.ru; smirnovda@yandex.ru)